Glycoconj J (2009) 26:477–493
DOI 10.1007/s10719-008-9198-5

Glycosylation-related genes are variably expressed depending on the differentiation state of a bioaminergic neuronal cell line: implication for the cellular prion protein

Myriam Ermonval · Daniel Petit · Aurélien Le Duc · Odile Kellermann · Paul-François Gallet

Received: 24 July 2008 / Revised: 17 September 2008 / Accepted: 1 October 2008 / Published online: 21 October 2008

Abstract A striking feature of the cellular prion protein (PrP^C) is the heterogeneity of its glycoforms, whose contribution to PrP^C function has yet to be defined. Using the 1C11 neuronal bioaminergic differentiation model and a glycomics approach, we show here a correlation between differential PrP^C *N*-glycosylations in $1C11^{5\text{-HT}}$ serotonergic and $1C11^{NE}$ noradrenergic cells compared to their 1C11 precursor cells and a variation of the glycogenome expression status in these cells. In particular, expression of genes involved in *N*-glycan synthesis or in the modeling of chondroitin and heparan sulfate proteoglycans appeared to be modulated. Our results highlight that, the expression of glycosylation-related genes is regulated during bioaminergic neuronal differentiation, consistent with a participation of glycoconjugates in neuronal development and plasticity. A neuronal regulation of glycosylation processes may have direct implications on some neurospecific functions of PrP^C and may participate in specific brain targeting of prion strains.

Keywords PrP^C · *N*-glycosylation · Glycotranscriptome · Glycoconjugates · Neuronal differentiation

Introduction

The cellular prion protein, PrP^C, is a ubiquitous host encoded GPI-anchored glycoprotein, which is clustered at the level of lipid rafts and particularly abundant at the surface of neurons [1]. The cellular PrP^C exists under various isoforms and in particular glycoforms [2], which vary both in terms of occupancy of the two *N*-glycosylation sites and in the composition of the complex *N*-glycans attached to each of these sites [3, 4]. A natural cleavage of cell surface PrP^C leads to full length or truncated fragments, both being non-mono- or di-glycosylated and as many as 50 different glycans have been identified as attached to the prion protein [5, 6]. While neurodegeneration is associated to the conversion of PrP^C into an abnormal pathogenic scrapie form, PrP^{Sc}, the natural function of PrP^C and the relative contribution of the different isoforms, are yet to be solved.

Different roles have been attributed to PrP^C relating to its capacity to bind metal ions [7], to interact with membrane proteins [8, 9] and extracellular matrix components [10, 11], or to recruit intracellular effectors such as kinases involved in signaling pathways [12–16]. The variety of the interactors described today supports the hypothesis of a

Electronic supplementary material The online version of this article (doi:10.1007/s10719-008-9198-5) contains supplementary material, which is available to authorized users.

M. Ermonval · O. Kellermann
Différenciation Cellulaire et Prions,
Département de Biologie Cellulaire et Infections, Institut Pasteur,
75015 Paris, France

M. Ermonval · O. Kellermann
CNRS FRE 2937,
94800 Villejuif, France

D. Petit · A. Le Duc · P.-F. Gallet (✉)
Faculté des Sciences et Techniques, Génétique Moléculaire Animale, UMR 1061 INRA/Université de Limoges,
123 Avenue Albert Thomas,
87060 Limoges cedex, France
e-mail: francois.gallet@unilim.fr

Present address:
M. Ermonval (✉)
Unité de Génétique Moléculaire des Bunyavirus,
Département de Virologie, Institut Pasteur,
25 rue du Dr Roux,
75015 Paris, France
e-mail: mermonva@pasteur.fr

modulatory role of PrP^C in diverse cellular functions as part of dynamic protein complexes [17]. Although little is known about the participation of PrP^C *N*-glycosylations in such functions, an important regional heterogeneity of PrP^C glycoforms exists at the level of brain regions [18, 19], which may have implications both in terms of physiology and neuropathology of the prion [20].

In the present study we investigated the glycosylation status of PrP^C in the 1C11 bipotential neuronal differentiation model. The 1C11 precursor line has the capacity to differentiate into two exclusive neuronal pathways leading either to a complete serotonergic ($1C11^{5\text{-HT}}$) or noradrenergic ($1C11^{NE}$) phenotype [21]. This cellular model already allowed to identify a signaling function of the prion protein displaying a neurospecificity in the bioaminergic neuronal cells [14]. Depending on the onset of a PrP^C–Cav–Fyn complex, PrP stimulation by antibody ligation triggers ERK1/2 kinase activation in these bioaminergic neurons [16] and modulates effectors coupling and cross-talk of serotonergic receptors [22]. Signaling functions are known to mainly occur in lipid rafts [23]. It is thus conceivable that the environment of PrP^C could vary in membrane microdomains during 1C11 neuronal differentiation and be responsible for its neurospecificity. Indeed each differentiation program is accompanied by the onset of functions associated to neurotransmitter metabolism and to the implementation of specific receptors and transporters of the corresponding monoamines [21]. In this context, it was recently demonstrated that the tissue non specific alkaline phosphatase (TNAP) is induced during each of the 1C11 bioaminergic programs, and could be part of PrP^C complexes in lipid rafts of $1C11^{5\text{-HT}}$ and $1C11^{NE}$ neuronal cells (Ermonval *et al.* unpublished results). Such neurospecificity of PrP^C function and interaction would also be compatible with a contribution of prion glycosylation, through recruitment of particular glycoforms of PrP^C in membrane subcompartments and/or involvement of carbohydrate interactions with partners specific of the differentiated state.

We describe here that, PrP^C electrophoretic glycopatterns varied according to the bioaminergic differentiation state of the 1C11 cell line, and also to the localization of the protein in neuronal subcompartments (neurites versus cell bodies in $1C11^{NE}$ cells). We used a glycomics approach [24] to address the question whether this could reflect some variation in glycosylation activities during 1C11 neuronal differentiation. To this aim, the level of expression of 375 murine glycosylation-related genes that belong to the glycosyltransferase, glycosydase, glycosyltranslocase, lectin and sulfotransferase families, was tested by transcriptomic microarray analyses. As many as 44 different transcript-encoding enzymes involved in different glycosylation metabolisms, or in the synthesis of glycoproteins interacting with carbohydrate moieties, were differentially expressed in $1C11^{5\text{-HT}}$ and $1C11^{NE}$ bioaminergic neuronal cells, using 1C11 precursor cells as reference. Some of these genes were expected to have an impact on *N*-glycan structures carried by PrP^C and on potential PrP^C interactors. In addition, it adds information about the glycogenomes expression in bioaminergic neuronal cells. Evidences are accumulating for an essential role of various glycoconjugates in the development of the central nervous system [25] among which proteoglycan structures expressed in the brain could be an important feature of neuronal plasticity [26]. In this context, PrP^C has been shown to interact with heparan sulfate [11] and it is of interest that enzymes of the glycosaminoglycan (GAG) metabolism appeared to be particularly regulated in serotonergic and noradrenergic cells. The differential PrP^C glycosylation described in the present study highlights that important regulation of glycosylation-related gene expression takes place during the course of bioaminergic neuronal differentiation.

Material and methods

Cell culture and reagents

1C11 cells were grown in DMEM medium (Gibco) supplemented with 10% foetal calf serum (Seromed). Neuronal differentiation into serotonergic ($1C11^{5\text{-HT}}$) or noradrenergic ($1C11^{NE}$) cells was induced by addition of dibutyril cyclic AMP (d-cAMP) or addition of d-cAMP in presence of 2% DMSO, respectively, as previously described [21].

Mouse monoclonal antibodies to prion protein, unlabelled SAF32 and SAF83 labelled with peroxidase, were obtained from SPIBIO. They recognized an N-ter epitope (a.a. 79–92) and the C-ter region of PrP^C (a.a. 126–164) respectively.

Secondary reagents used for immunoblot detection, goat anti-mouse, goat anti-rabbit antibodies coupled to horseradish peroxidase (HRP), or streptavidin HRP to detect immunoprecipitated biotinylated proteins were purchased from Southern Biotechnology.

For glycan analysis, glycosidases (neuraminidase, *N*-glycosidase and *O*-glycosidase) were purchased from Glyko (San Leandro, CA, USA) and the biotinylated lectin: *Aleuria aurantia* (AAL), *Canavalia ensiformis* (Con A), *Maakia amurensis* (MAL1), *Sambucus nigra* (SNA), *Vicia villosa* (VVL), Wheat germ agglutinin (WGA), were from Vector Laboratories.

Unless indicated, the reagents were purchased from Sigma.

Preparation of lipid rafts (GSL) and fractionation of neurites and cell bodies

Purification of glycosphingolipid (GSL) rich complexes was performed according to Clausse [27]. Briefly, cells

washed in PBS were scraped on ice before being disrupted and homogenized at 4°C in 3 mL MBS (MES buffered saline): 25 mM MES pH 6.5; 150 mM NaCl, containing 1% Triton X-100 (TX-100) and protease inhibitors (Complete™ from Roche) and orthovanadate phosphatase inhibitor. The cell homogenate was clarified and brought to a volume of 4 mL at 40% sucrose in MBS/TX-100, then overlaid with 4.5 ml of a 30% sucrose solution in MBS (without TX-100) and with 2,7 mL of a third layer of MBS without sucrose. The step-gradient was centrifuged for 20 h at 180,000×*g*. The lipid rafts containing GSL complexes were recovered as an opalescent band at 5 mm beneath the 0–30% layers interface. They were harvested and diluted to a volume of 3 mL in MBS. GSL complexes were then pelleted by centrifugation for 1 h at 300,000×*g*. Such raft preparations were dissolved in 6% SDS-RIPA buffer (150 mM NaCl, 25 mM Tris-HCl pH 7.4, 5 mM EDTA, 0.5% Na-DOC and 0.5% NP40).

Cell fractionation of neurites and cell bodies was performed as described [28]. Briefly $1C11^{5\text{-HT}}$ or $1C11^{NE}$ fully differentiated cells were scraped and broken through a needle. This preparation was then layered on a 20% sucrose cushion in PBS. Upon centrifugation at 1,000×*g* for 5 min, the cell bodies were pelleted and submitted to a second purification on a sucrose cushion. The neurites were recovered on the top of the sucrose solution. Cell debris were thus eliminated and neurites collected from the supernatant by centrifugation at 105,000×*g* for 30 min. For western blot analysis, the different lysates were prepared in NET buffer (150 mM NaCl, 50 mM Tris HCl pH 7.4, 5 mM EDTA) containing 1% TX-100 (Calbiochem) and protease inhibitors. Quantification of proteins was carried out by dosage with the BCA kit from Pierce.

1D- and 2D-gel electrophoresis and immunodetection by western blot analysis

For 1D gel analysis, cell lysates (15 μg of total extract or 1 μg of raft proteins) were run on SDS-PAGE (Bio-Rad). After protein transfer onto nitrocellulose membrane (Amersham), the membrane was blocked with 1% gelatin in PBS 0.1% Tween 20 (PBST). The blot was then reacted with the specific primary antibody *i.e.* SAF32 (10 μg/mL). Immunoblots were revealed by specific secondary antibodies coupled to HRP (1/10,000) before ECL staining. For glycosylation studies, glycosidase treatments were performed prior to electrophoresis. Around 15 μg of proteins were digested with either neuraminidase (5 μU) to cleave terminal sialic acid or with a PNGaseF (1 μU) and *O*-glycosidase (2 μU) mixture for complete removal of glycans.

For 2D gel analysis, PrP^C was first immunoprecipitated from biotinylated membrane proteins. 1C11 precursor cells or their bioaminergic neuronal progenies grown in monolayer were washed twice with PBS Ca^{2+}/Mg^{2+} then incubated for 30 min at 4°C with EZ-link™-sulfo NHS-LC-biotin (Pierce) at a concentration of 0.5 mg/ml in PBS. Biotinylated cells were washed then lysed in NET buffer at 1% TX-100. Immunoprecipitation was performed using protein A sepharose beads (GE Healthcare) coupled to SAF32 anti-PrP^C antibodies, which were incubated overnight at 4°C with biotinylated lysates. Beads were washed 4 times in high salt buffer (NET, 1% TX-100 in 0.5 NaCl), then twice in Hepes 40 mM before elution with a denaturating 9.5 M urea buffer containing 2% TX-100, 5% β-mercaptoethanol and 2% ampholytes in a range of pH 3 to 10. Prior to separation, samples were alkylated and incubated on preformed strip gradients (Zoom system Invitrogen). Isoelectric focusing was obtained by applying 500 V for 15 min then 750 V for 4 h 30 min. Focused proteins on the strip gel were further reduced and alkylated before being submitted to a second separation on a 4–12% SDS-PAGE gradient (Invitrogen). Western blotting was then performed as above, except that biotinylated PrP^C was detected with streptavidin–peroxidase conjugate at 1/100,000 dilution.

Glycosylation related-gene expression analysis by TLDA technique

Total RNAs were prepared from 1C11 precursor cells and from fully differentiated neuronal cells, *i.e.*: $1C11^{5\text{-HT}}$ serotonergic cells at day 4 or $1C11^{NE}$ noradrenergic cells at day 12 of differentiation, using the RNeasy midi kit (Qiagen Inc, Hilden, Germany) according to the manufacturer's instructions. RNA quantity and quality were assessed using the Agilent 2100 Bioanalyzer (Agilent Technologies, Massy, France) and 1% agarose gel electrophoresis. DNase treated RNA (3 μg) from each sample was reverse transcribed using random hexamers and the cDNA Archive Kit (Applied Biosystems, Courtaboeuf, France), following the supplier's recommendations.

Quantitative PCRs were performed using custom-made TLDA (Taq-Man Low Density Array) cards focused on glycosylation (Applied Biosystems). Microfluidic cards consisted of 384 microwells loaded with eight ports each leading to 48 wells by capillarity. Each well contained a set of pre-defined primers and a fluorescent TaqMan probe (FAM-labelled) to allow amplification on each card of 375 different murine glycosylation-related genes and housekeeping genes used as control (18S RNA, *TfIId* transcription factor [29],…). The list of the tested genes is given in supplementary data (Table S1). Normalization of cDNA levels in the different wells was done using the 18S RNA as reference. Two ng of cDNA were distributed in each well by brief centrifugation (2 min at 260×*g*). After a first step at

95°C for 10 min, amplification reaction was carried out by performing 40 cycles of denaturation, annealing/extension steps as follows: 15 s at 95°C, 1 min at 60°C. Changes in the fluorescence of the TaqMan probe were monitored on the ABI PRISM 7900HT sequence detector system and quantified by the SDS 2.2 software (Applied Biosystems) according to the $\Delta\Delta$Ct method. Briefly, ΔCt corresponds to the threshold cycle (Ct) for each gene minus that of the endogenous 18S RNA internal control. Comparative gene expression $\Delta\Delta$Ct represents the ΔCt for each gene in a given condition ($1C11^{5\text{-HT}}$ or $1C11^{NE}$) minus ΔCt value of the same gene in the exogenous control condition (1C11) serving as calibrator. Relative quantification (RQ) of the genes in a sample was determined according to the equation $2^{-\Delta\Delta Ct}$, a relative quantity of one being assigned to the genes in 1C11 exogenous control samples.

In order to assess the reproducibility of the data, RQ values were determined using three independent RNA preparations numbered 1 to 3 and each preparation included the different cell states: 1C11, $1C11^{5\text{-HT}}$ and $1C11^{NE}$. Two sets of TLDA were independently run for quantification of glycosylation-related gene expression, the first with preparation n°1 and the second with preparations n°2 and 3. In this second set it was then allowed to match gene expression levels in the differentiated states for preparation n°2 or 3 with the ones of 1C11 preparations n°3 or 2 respectively. All the combinations obtained from the two TLDA sets, led to five different experimental conditions in each differentiation pathway, as schematized in the insert of Fig. 3 (5HT-1 to 5 and NE-1 to 5). Thus, RQ values 1 to 3, corresponded to gene expression changes in the $1C11^{5\text{-HT}}$ and $1C11^{NE}$ differentiated states using as reference 1C11 RNA sample of the corresponding experimental condition (1–1, 2–2, and 3–3). The RQ values numbered 4 and 5 were derived by matching the differentiated state $1C11^{5\text{-HT}}$ or $1C11^{NE}$ in preparation n°2 with 1C11 preparation n°3 (2–3) and differentiation state n°3 with 1C11 n°2 (3–2), respectively. Only the mean RQ value of the five experimental conditions is given for each gene in each pathway (see Table 2).

Statistical significance of gene expression data was evaluated by using the Student test. For each gene, the mean RQ value obtained either in the serotonergic or the noradrenergic differentiation pathway was compared to fixed values used as reference. The fixed values correspond to the mean of expression change of all genes in each of the five combinations for a given differentiation path. The significance of each gene expression level was assessed, by comparing the five experimental RQ values with the five reference values using a Student test under Windows™ Excel for calculation. Differences were considered as significant at a $P<0.05$. The relevance of fold changes was also evaluated by calculating the false discovery rate (FDR) using SAM (Significance Analysis of Microarrays) version 3.0 [30]. The T-statistics with 1,000 permutations were applied on the log2 transformed data.

PCA on total data

To uncover trends of the data obtained by TLDA, we performed a global analysis of log-transformed expression levels of the 375 selected genes in the ten experimental conditions tested, by using a principal component analysis (PCA) with PAST vers. 1.78 [31] This mathematical procedure reduces the number of possibly correlated variables (five combinations in each of the two bioaminergic differentiation pathways for the 375 genes) into a smaller number. Ideally, most of the data informations (ten dimensions for expression fold changes of the 375 genes) are projected in a 2D-space defined by the two principal components P1 and P2, which are synthetic axes expressing the percentage of variance of the data. Indeed, PCA extracts the direction where the cloud of values is more extended, constituting the first component or principal component (P1). The next direction (P2) is orthogonal to the first one. The cloud of points reflects expression level of each gene according to their position to the vectors, which indicate orientation of variation in each combination. Vectors correspond to most representative expression profiles of the data in a given combination. Therefore, samples belonging to a same pattern are expected to be grouped in a similar area as in the case of vectors 5HT-1 to 5HT-5, corresponding to the serotonergic differentiation pathway, and NE-1 to NE-5 vectors corresponding to noradrenergic differentiation (see above the TLDA method section and Fig. 3 inset for vector numbering).

Principal component analysis also allows drawing a dendrogram representation of hierarchical links between the different experimental conditions. It was obtained by calculating the euclidian distances of the projection of vectors on components 1 and 2. Significance of the correlation was then assessed by the Bonferroni test [32].

PCR analysis of gene expression

Each PCR reaction was carried out using 210 ng of cDNA amplified by 10 pmol of each set of primers (see Table 1) in PCR master mix (Abgene). Samples were treated at 95°C for 10 min followed by 35 cycles at 95°C for 10 s, 60°C for 10 s and 72°C for 30 s each, then by a final step of extension at 72°C for 2 min. PCR amplification products were analyzed in a 3% (*w*/vol) agarose gel. For each gene tested, level of expression was evaluated in 1C11, $1C11^{5\text{-HT}}$ and $1C11^{NE}$ cDNA preparations and a negative control without cDNA was included.

Table 1 Sequences of primer sets used in RT-PCR and size of corresponding amplified fragments

Gene name	Accession number NM	Forward primer	Reverse primer	Amplicon size—bp
B3gnt3	28189	GGAGTTGACATCCCCTAGCTCAT	CCCTCACTTTGAACTTCTCCTTGA	79
B4galnt2	8081	GGTTTTGATCCCATCTTGCAA	GTGTTGGCCCGGTATTTGTC	176
Chgn	172753	CCTGCTCTTTTTCTGTGATGTAGACA	TTCTTCCCTGGCTGTGTGTTC	84
Chst3	16803	CGCACGGGTTCCTCGTT	CAGGTCGCATAGCAACAACTG	177
Chst5	19950	GGCAGCCAGCCTCCTACTAAA	TGCGATTGCATGGTATGATCA	75
Chst8	175140	TTCTCGTCCATCCTGCTGTTT	GGTGAATCTCGTGTGCCCTTT	176
Extl1	19578	GTTGCGTTTGGCACGTTTC	ACCAGGCAGAGATGCAGAGAA	83
Fut4	10242	GGACCGACTCGGATGTCTTC	GCCGACTCAGCTGGTGGTA	177
Gbgt1	139197	TGCCATTCACCCAGGCTATT	GGAAACTTGCCTGCGTTCAT	67
Gyltl1b	172670	GCTTCTACTGCCACCCAAGTG	TGTTTCTGGCTACGGCATCAG	75
Has1	8215	CACCAACCGAATGCTTAGCA	GGCGTCTCCGAGTAGCATCT	72
Has2	8216	TCCTTGCTGCATGAATTTGTG	CGTCACCAAAACTGCATTGG	73
Hs3st3a1	178870	TTGGCCTTCCAGTTTTCTTTCTC	CCCTGTGCATGCTGAGTATCTTAG	78
Itga2	8396	CCATCACAAAGGGCATCTTGA	GCTGAACCAAACCGAGCATT	79
Itga2b	10575	GGGCAACCCCATGAAAAAG	GACACGGACTCGCCAGCTT	87
Lctl	145835	TCGACAACCCCGACGATATT	TGGCAAACCAACCGAGACA	66
Lfng	8494	ACTGCACCATTGGCTACATTGTA	GGTTCTCTAGGTGGGAGTGGAA	85
Lgals7	8496	CGTGGGCACTGTCATGAGAAT	CCTCACCGCATAGCAGGTTT	80
Mgat3	10795	TTGATGTGGGCCAAGAAGCTA	GTCCCGCATGTCTGAGGAA	83
Mgat4a	173870	TCCACAGCGGCAATCAAGA	GATCCACAATTCCCTCTGCAA	177
Mgc4655	178879	AGTCATGGGAGTGCCACACA	ACCTGCCCCAGCTGTCTGT	65
Neu2	15750	GCTGTCCCTGGGCGTGTAT	CCAGGACCCACAGCAAATGT	176
Olr1	138648	CCTGTTGCCGCATGAAAGA	GGACGAGCTTTGCCTTTGAG	76
Siglec10	172900	CCCAGATCCCACATCATCCT	TCAGGCGGGAGAAGTTGAGA	89
Slc2a6	172659	CCCCTCAGCCATTGGCTAT	CAAAGCCCGTCAGCATCCT	83
St3gal1	9177	AGAGAAGCCGATCTGTAGCCTTT	CCTCTAGGTTCTCAATATCCACTGTGTA	186
St3gal5	11375	TCGATGTGCAGCTAGTGTTTTCA	AAAGTCCTTCCAATCCCATTCTT	176
St6galnac2	9180	TCACCGTGAACACCATGAAGA	TCTGCCCTTGTGGCACAGA	75
TfIId	13684	TTGACCTAAAGACCATTGCACTTC	CATGATGACTGCAGCAAATCG	74
Thbd	9378	GTCACCTGCGCAAGAAGCA	ACCTCCTTGGCGGAAGATG	74
Ugcg	11673	CAGGAGGGCTCATAGCCTTTG	AACCTCGGTCGGCTATTGC	75
Ust	177387	GAAGCTTGCCGAGATCAAGCT	GAGCGATACCTGGGAATGGA	70
Vcam1	11693	GGGACGATTCCGGCATTTA	CGGGCACATTTCCACAAGT	177

Lectin reactivity of PrP^C measured by capture-ELISA

Quantification of PrP^C in different cell lysates was achieved by sandwich ELISA using as standard reference normal mouse recombinant PrP ($MoPrP^{rec}$) from Alicon. In brief, 96-well microplates were coated with SAF32 antibodies at 7.5 μg/ml in phosphate buffer pH 8.5, saturated with 1% gelatin in PBS and reacted with dilutions of $MoPrP^{rec}$ or cell lysates. Captured PrP was detected with SAF83-HRP (1/1,000) conjugate, then revealed with ABTS substrate kit (Vector laboratories). Titration curves were obtained by measuring absorbance at 405 nm as a function of MoPrP or cell lysate dilution.

Carbohydrates carried by PrP^C from bioaminergic $1C11^{5\text{-HT}}$ and $1C11^{NE}$ differentiated cells and the neuroepithelial 1C11 precursor cell lysates, were compared using biotinylated lectins with different specificities: 1 μg/ml AAL specific for fucose, 1 μg/ml ConA specific for glucose and mannose, 13 μg/ml MAL1 specific for galactose, 1 μg/ml SNA specific for sialic acid, 13 μg/ml VVL specific for *N*-acetylgalactosamine, and 15 μg/ml WGA (*N*-acetylglucosamine). Lectin interacting with captured PrP^C were detected by use of streptavidine–peroxidase (1/100,000) that was revealed with the ABTS substrate kit. For each condition, a test was performed in triplicate. Quantification of PrP in the cell lysates was obtained by extrapolation from regression curves of purified $MoPrP^{rec}$. Lectin reactivities were expressed as arbitrary units corresponding to mean value of the OD at 405 nm/ng of PrP^C.

Sulfated GAG quantification

Sulfated GAGs were quantified according to Barbosa [33] with slight modifications. Briefly, 1C11 undifferentiated cells and, $1C11^{5\text{-HT}}$ and $1C11^{NE}$ fully differentiated

neuronal cells were washed twice with PBS containing Ca^{2+} and Mg^{2+} before being scraped, then pelleted by centrifugation for 5 min at 700×*g*. The pellets were suspended in 1 mL of lysis buffer containing K_2HPO_4 100 mM pH 8.0, TX-100 1% and incubated for 10 min at 4°C. The lysates were centrifuged for 30 min at 13,000×*g* to discard DNA and protein digestion was performed by an overnight incubation at 56°C with 50 μg/mL of proteinase K (PK). Upon inactivation of PK by heating for 10 min at 100°C, the digested samples were filtered through an Ultrafree-MC (Millipore, Bedford, MA) filter to remove residual DNA. One mL of DMMB at 34 mg/L (in 5% ethanol, 0.2 mM GuHCL, 2% sodium formate and 0.15% formic acid) was added to 25 μL of PK-treated samples. The mixture was vigorously vortexed for 30 min to promote complexation, then centrifuged for 30 min at 13,000×*g*. The pellets containing the GAG–DMMB insoluble complexes were dissolved in 1 mL of the decomplexation solution (50 mM sodium acetate pH 6.8, 10% propan-1-ol, 4 M GuHCl) and absorbance was monitored at 656 nm. To evaluate the content in chondroitin sulfate, 100 μL of PK-treated samples were reacted for 1 h with sodium nitrite (100 μL at 5%) and acetic acid (100 μL at 33%) to eliminate heparan sulfate. This reaction was stopped by addition of ammonium sulfamate (100 μL at 12.5%). A 100 μL fraction of this mixture was then complexed to DMMB as above for CS determination and absorbance was measured at 656 nm. Total or chondroitin sulfated GAG levels were calculated from a calibration curve obtained with a mixture of chondroitin sulfate A, C and D used as standard. Sulfated GAGs were expressed as μg of GAG/μg of protein in each sample.

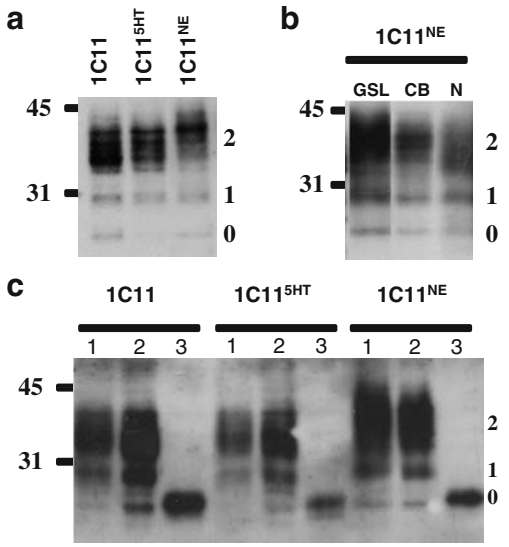

Fig. 1 PrP^C present in different neuronal conditions was detected by western blotting with SAF32 anti PrP antibody. Position of PrP^C migrating as non-, mono- or di-glycosylated forms, is indicated by *0*, *1* and *2* respectively on the right side of the blots. In **a** are compared the glycoprofiles of PrP^C from 1C11 precursor cells with the one from $1C11^{5\text{-HT}}$ serotonergic and $1C11^{NE}$ noradrenergic progenies, illustrating the shift of the di-glycosylated forms towards more complex structures in fully differentiated cells. In **b** is shown profiles of PrP^C from different fractions of $1C11^{NE}$ noradrenergic cells where GSL fraction corresponds to lipid rafts, CB to the cell bodies and N to the neurites subcellular compartment. In **c**, PrP^C from lysates of undifferentiated 1C11 cells, of $1C11^{5\text{-HT}}$ serotonergic and $1C11^{NE}$ noradrenergic differentiated cells, has been left untreated (*lanes 1*), digested with neuraminidase (*lanes 2*) to remove terminal sialic acid, or fully deglycosylated with a mixture of peptide *N*-glycanase and *O*-glycanase (*lanes 3*). Under this latter condition PrP^C migrates at the level of the non glycosylated PrP^C isoform found in the other samples (compared *lanes 3* with non glycosylated native forms in *lanes 1 and 2*). Standard molecular weights migration is indicated on the *left side of each panel*

Results

Electrophoretic glycosylation patterns of PrP^C vary with the differentiation state of 1C11 neuronal cells

PrP^C migrates in one dimensional gel (1D-gel) as three major species of about 27, 30 and 38 kDa apparent molecular mass, corresponding to non-, mono- or di-glycosylated forms, respectively, the latter being very heterogeneous in size (Fig. 1). As expected, carbohydrates carried by PrP^C result from N-glycosylation since O-glycanase treatment alone had no effect on the PrP^C glycoprofile (data not shown). This is also illustrated by the fact that deglycosylated PrP^C upon treatment with P-NGase alone (data not shown) or in combination with O-glycosidase (Fig. 1c, lanes 3), migrated at the level of the non glycosyated 27 kDa native form. However, PrP^C electrophoretic profiles differed between 1C11 precursor cells and the $1C11^{5\text{-HT}}$ serotonergic and $1C11^{NE}$ noradrenergic derived cells. Indeed, di-glycosylated PrP^C species in $1C11^{NE}$ cell lysate exhibited the highest molecular weights (Fig. 1a), then, although faster migrating, a greater proportion of PrP^C still displayed higher molecular weights in $1C11^{5\text{-HT}}$ than in 1C11 cells (Fig. 1a). Interestingly, different profiles also occurred depending on the subcellular location of PrP^C in $1C11^{NE}$ cells. Figure 1b illustrates such variation of PrP^C glycopatterns in cell bodies (CB) and in neurites (N) of $1C11^{NE}$ cells. The shift of PrP^C towards more complex glycan structures, quite visible in CB fraction, was also present in $1C11^{NE}$ lipid rafts (GSL). In addition to complex *N*-glycans of higher molecular mass in noradrenergic cells, an increase in the number of terminal sialylations was supported by a slight size reduction of PrP^C from $1C11^{NE}$ cells upon neuraminidase treatment. However, a faster migration of PrP^C was not distinguishable under such conditions in $1C11^{5\text{-HT}}$ (Fig. 1c).

Considering the great heterogeneity of the *N*-glycans carried by PrP^C [6], 1D-gels are only partly informative. In an attempt to better visualize such post-translational modifications of PrP^C, we performed a two-dimensional gel analysis (Fig. 2). Biotinylated membrane PrP^C was immunoprecipitated then separated, based on its isoelectric point, using a large pH range (from 3 to 10) in order to identify as many glycosylated species as possible. Indeed, PrP^C from 1C11, $1C11^{5\text{-HT}}$ and $1C11^{NE}$ appeared as many spots in such 2D-gels. Of note, in contrast to our 1D-gel analyses revealing all PrP^C forms found in total extracts, di-glycosylated species which are preferentially transported to the cell surface were, as expected, predominant in the 2D-gels. The 2D profiles revealed differences both in terms of intensity and distribution of PrP^C glycoforms in the three cell states. In 1C11 precursor cells, the uppermost forms of full length di-glycosylated PrP^C forms (31 to 43 kDa) span pI values from pH 6 to 7.5. In both $1C11^{5\text{-HT}}$ serotonergic and $1C11^{NE}$ noradrenergic progenies, additional spots exhibiting higher molecular weights and covering more acidic pI values in the range of pH 5.5 to pH 6 were also evidenced. These more acidic PrP^C species, which migrated as di-glycosylated forms of higher molecular weights in $1C11^{NE}$ cells fit well with the molecular mass reduction of PrP^C observed upon neuraminidase treatment (Fig. 1c).

These results reveal that different patterns of PrP^C glycoforms are present in 1C11 precursor cells and the serotonergic and noradrenergic neuronal progenies. In particular, size and charge variations of PrP^C *N*-glycans are noticeable in bioaminergic neuronal cells.

Glycosylation-related gene expression profiling of $1C11^{5\text{-HT}}$ and $1C11^{NE}$ neuronal cells as compared to 1C11 precursor cells

The changes in PrP^C *N*-glycosylation relating to 1C11 neuronal differentiation states, prompted us to address the question whether this could reflect differences in expression of genes involved in glycosylation processes.

Gene expression patterns were determined by a glyco-transcriptomic approach performed on mRNA purified from 1C11 precursor cells or fully differentiated neuronal cells: *i.e.* $1C11^{5\text{-HT}}$ serotonergic cells at day 4 and $1C11^{NE}$ noradrenergic cells at day 12 of the differentiation programs, respectively. For each cellular condition, reproducibility was assessed by submitting three independent preparations, in triplicate, to TLDA microarray designed to identify differentially expressed glycosylation genes. Description of the genes is given in the supplementary data (Table S1). Among the 375 mouse glycosylation-related genes tested, around 50 genes exhibited a significant (four fold change) and statistical ($P<0.05$) variation (Table 2). The False Discovery Rate (FDR) analysis applied to these 50 genes was found to be of 4.81%, also supporting the validity of our results. A fold difference representation of gene expression profiles by a principal component analysis

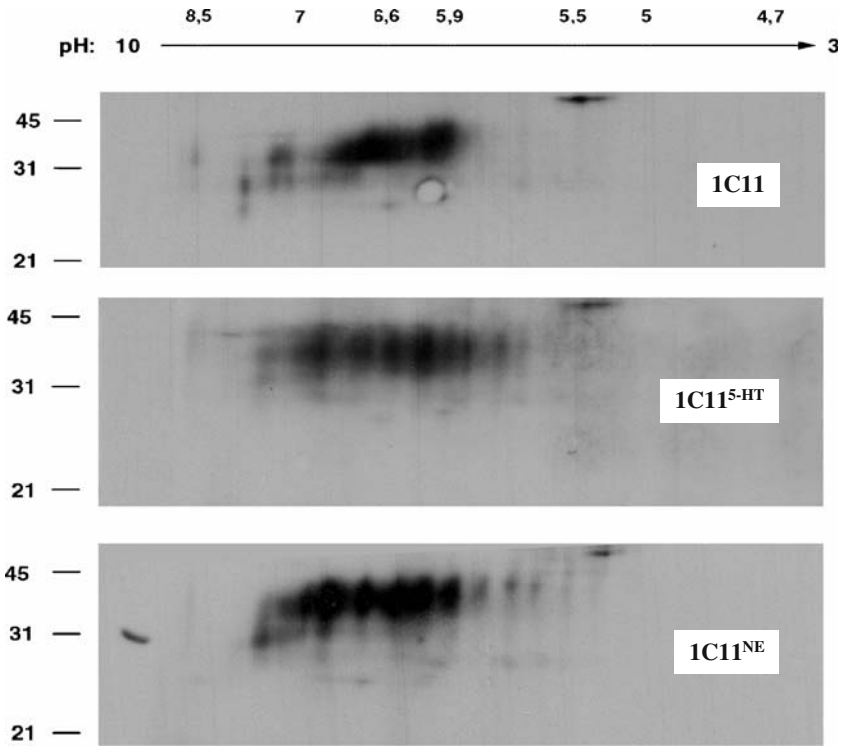

Fig. 2 PrP^C immunoprecipitated from 1C11, $1C11^{5\text{-HT}}$ or $1C11^{NE}$ cells was analyzed by 2D-gel and then revealed by western blotting using streptavidine-HRPO in order to visualize *N*-glycan species associated to biotinylated PrP^C at the cell surface. The pH range of the first dimension is indicated at the *top of the blots*. Standard molecular weights are indicated on the *left side of each panel*

Table 2 Description of genes with increased and decreased expression during 1C11 neuronal differentiation

Gene	$1C11^{5\text{-HT}}$ RQ (p student)	$1C11^{NE}$ RQ (p student)	Protein	Function
INCREASED EXPRESSION				
St3gal1	9,4 (2,9 E-06)	5,3 (2,0 E-04)	ST3 β-galactoside α-2,3-sialyltransferase 1	Glycosyltransferase: SiaT, NeuAc-α-3-Gal-β-3-GalNAc structure on O-glycans and gangliosides
St6galnac2[a]	1,1 (9,0 E-01)	0,320 (8,5 E-03)	ST6 (α-N-acetyl-neuraminyl-2,3-β-galactosyl-1,3)-*N*-acetylgalac tosaminide α-2,6-sialyltransferase 2	Glycosyl transferase SiaT
Chgn	8,9 (1,6 E-04)	19,3 (2,2 E-06)	Chondroitin β1,4 *N*-acetylgalactosaminyltransferase	Glycosyltransferase: GalNAcT, Chondroitine linker synthesis
Mgat4a[b]	1,5 (7,0 E-01)	6,7 (2,1 E-02)	Mannosyl (α-1,3-)-glycoprotein β-1,4-*N*-acetylglucosaminyltransferase, isozyme A	Glycsoyltransferase:GlcNAcT, triantenary N-glycan structure
Fut4	5,7 (3,5 E-03)	1,6 (6,4 E-1)	Fucosyltransferase 4 (α (1,3) fucosyltransferase, myeloidspecific	Glyosyl transferase: FucT, Lewis X/ SSEA-1 and VIM-2 antigens
Ugcg[b]	4,1 (2,1 E-4)	2,0 (1,1 E-01)	UDP-glucose ceramide glucosyltransferase	Glycsoyltransferase: GlcT first step of glycosphingolipid synthesis
B4galnt2	0,8 (1,8 E-01)	57,5 (1,4 E-04)	β-1,4-*N*-acetylgalactosaminyl transferase 2	Glycsoyltransferase: GalNAcT, Sd(a) antigen (Sia-α2,3-[GalNAc-β1,4]Gal-β1,4-GlcNAc) synthesis
B3gnt3	1,5 (3,3 E-01)	4,5 (1,0 E-03)	UDP-GlcNAc:βGal β-1,3-*N*-acetylglucosaminyltransferase 3	Glycsoyltransferase: GlcNAcT type 2 oligosaccharides synthesis
Has1	96,0 (4,1 E-08)	1,3 (7,4 E-01)	Hyaluronan synthase 1	GAG synthesis: hyaluronan/hyaluronic acid (HA) synthesis
Ugdh	4,5 (1,7 E-03)	2,3 (1,2 E-01)	UDP-glucose dehydrogenase	Deshydrogenase: converts UDP-glucose to UDP-glucuronate, Substrat for GAG synthesis
Ust[c]	11,6 (2,4 E-06)	10,1 (6,7 E-06)	Uronyl-2-sulfotransferase	Sulfotransferase: CSPG sulfatation
Hs3st3a1	5,3 (5,0 E-03)	5,1 (2,2 E-03)	Heparan sulfate (glucosamine) 3-O-sulfotransferase 3A1	Sulfotransferase: HSPG sulfatation
Chst5	4,2 (2,5 E-02)	4,3 (6,5 E-03)	Carbohydrate (*N*-acetylglucosamine 6-O) sulfotransferase 5	Sulfotransferase: SLeX synthesis on mucin-type receptor
Chst8	2,5 (1,4 E-02)	307,5 (4,5 E-06)	Carbohydrate (*N*-acetylgalactosamine 4–0) sulfotransferase 8	Sulfotransferase: GalNAc sulfatation of N- and O-glycans
Slc5a3	5,4 (3,1 E-03)	4,4 (1,2 E-01)	Solute carrier family 5 (inositol transporters), member 3	Sugar transporter: inositol transporter
Neu2	25,7 (5,7 E-05)	2,6 (4,0 E-02)	neuraminidase 2 (cytosolic sialidase)	Glycan hydrolysis: terminal sialic residues in oligosaccharides, glycoproteins, glycolipids
Masp1	6,5 (1,6 E-03)	13,1 (2,7 E-4)	Mannan-binding lectin serine peptidase 1 (C4/C2 activating component of Ra-reactive factor)	CBP-lectin with peptidase activity
Clec3b	12,4 (7,9 E-03)	0,3 (2,9 E-02)	C-type lectin domain family 3, member B	CBP-Lectin:Tetranectin (lectin) binds to plasminogen
Pecam1	0,9 (3,2 E-01)	6,3 (6,4 E-03)	Platelet/endothelial cell adhesion molecule (CD31 antigen)	Adhesion molecule; non siglec lectin
Itga2b[a]	4,3 (4,8 E-03)	4,8 (2,8 E-03)	Integrin, α 2b (platelet glycoprotein IIb of IIb/IIIa complex, CD41 antigen)	Adhesion molecule: membrane receptor for fibrinogen, plasminogen,É
Mcam	4,3 (5,9 E-4)	5,3 (1,2 E-02)	Melanoma cell adhesion molecule	Adhesion molecule: endothelial and neural crest cells
Thbd	11,8 (1,7 E-4)	4,7 (3,3 E-03)	Thrombomodulin	Receptor: coagulation factor upon complexing with thrombin
DECREASED EXPRESSION				
Mgat3[b]	0,482 (8,2 E-04)	0,345 (9,7 E-03)	Mannosyl (β-1,4-)-glycoprotein β-1,4-*N*-acetylglucosaminyltransferase	Glycosyl transferase GlcNAc T, elongation of trimannosyl core of N-linked sugar chains

Table 2 (continued)

Gene	$1C11^{5\text{-HT}}$ RQ (p student)	$1C11^{NE}$ RQ (p student)	Protein	Function
Lfng	0,118 (5,9 E-07)	0,034 (1,5 E-04)	LFNG O-fucosylpeptide 3-β-*N*-acetylglucosaminyltransferase	Glyosyl transferase: GlcNAcT, elongation of O- linked fucose of Notch
Galnt3	0,508 (1,7 E-03)	0,081 (2,2 E-03)	UDP-*N*-acetyl-α-D-galactosamine: polypeptide *N*-acetylgalactosaminyltransferase 3 (GalNAc-T3)	Glyosyl transferase: GalNAcT, initial step in O-glycan synthesis
Gbgt1	0,436 (4,3 E-04)	0,142 (1,7 E-04)	Globoside α-1,3-*N*-acetylgalactosaminyltransferase 1	Glyosyl transferase: GalNAcT, synthesis of some glycolipid
St3gal5	0,122 (1,1 E-06)	0,324 (4,9 E-03)	ST3 β-galactoside α-2,3-sialyltransferase 5	Glyosyl transferase: SiaT, ganglioside GM3 synthesis
St6gal1	0,572 (2,4 E-02)	0,184 (4,8 E-04)	ST6 β-galactosamide α-2,6-sialyltranferase 1	Glyosyl transferase: SiaT, from CMP- sialic acid to galactose containing substrates
Extl1[b]	0,647 (1,3 E-02)	0,307 (5,7 E-04)	Exostoses (multiple)-like 1	Glycosyltransferase: synthesis of GlcNAc-GlcA disaccharide unit of GAG
B3gnt7	0,651 (7,4 E-02)	0,189 (7,3 E-03)	UDP-GlcNAc:βGal β-1,3-*N*-acetylglucosaminyltransferase 7	Glyosyl transferase: GlcNAcT, keratane sulfate biosynthesis
Has2	0,994 (4,2 E-01)	0,035 (6,0 E-05)	Hyaluronan synthase 2	GAG synthesis; hyaluronan/hyaluronic acid (HA) synthesis
Chst3	0,045 (3,8 E-05)	0,004	Carbohydrate (chondroitin 6) sulfotransferase 3	Sulfotransferase: CSPG sulfatation. Can also sulfate keratan
Gyltl1b[b]	1,890 (3,0 E-01)	0,185 (3,3 E-03)	Glycosyltransferase-like 1B	Glyosyl transferase activity: glycosylation of α-dystroglycan and glycosphingolipid
Mgc4655[a]	0,551 (3,2 E-03)	0,212 (3,2 E-04)	Hypothetical protein MGC4655	Glycosyl transferase family, GalT activity:
Slc2a6[a]	0,022 (8,8 E-08)	0,104 (6,1 E-05)	Solute carrier family 2 (facilitated glucose transporter), member 6	Sugar transporter: glucose transporter
Lctl	0,103 (1,0 E-07)	ND*	Lactase-like	Glycan hydrolysis glycosyl hydrolase 1 family, Klotho subfamily
Siglec10	0,056 (5,5 E-07)	0,039 (9,3 E-04)	Sialic acid binding Ig-like lectin 10	CBP-lectin: mediates sialic-acid dependent binding to cells
Clec11a	0,086 (6,3 E-05)	0,065 (8,3 E-04)	C-type lectin domain family 11, member A	CBP-lectin
Lgals2	0,224 (1,1 E-04)	0,070 (8,6 E-05)	Lectin, galactoside-binding, soluble, 2	CBP-lectin binds galactose
Lgals7	0,390 (1,0 E-02)	0,016 (9,5 E-05)	Lectin, galactoside-binding, soluble, 7 (galectin 7)	CBP-lectin binds galactose
Olr1	0,117 (1,4E-05)	0,09 1 (3,1 E-05)	Oxidized low density lipoprotein (lectin-like) receptor 1	OxLDL lectine like receptor
Vcam1	0,145 (7,6 E-06)	0,001 (2,2 E-08)	Vascular cell adhesion molecule-1	Cell adhesion molecule
Itga11	1,837 (3,3 E-02)	0,123 (7,0 E-05)	Integrin, α11	Integrin α11/β1 is a receptor for collagen
Itga2	0,262 (4,6 E-04)	0,145 (1,9 E-03)	Integrin, α2 (CD49B, α2 subunit of VLA-2 receptor)	Integrin α2/β1 is a receptor for laminin, collagen, fibronectin É

[a] RQ (relative quantity) values are different from expression level obtained by PCR fin Fig. 6
[b] Problem of significance either of the p value or of the fold change but confirmed by PCR
[c] Not confirmed by PCR. Name of genes tested by PCR are in bold

(PCA) and clustering according to correlation tests is given in Fig. 3. Each oriented vector indicates the direction of the variation of gene expression in one differentiated state ($1C11^{5\text{-HT}}$ or $1C11^{NE}$) for the five experimental conditions described in methods. The efficiency of PCA was satisfactory since 78% of all the information from TLDA data were recovered on this graph (63.4% in component 1 and 15.2% in component 2). Genes whose expression was not significantly modified according to our criteria, appeared as a cloud of points at the center of the graph. In order to better visualize the genes of interest, this bulk of genes was not represented. A good correlation between experiments in each serotonergic and noradrenergic pathway was obtained as shown both by the small angles between vectors (Fig. 3) and by the dendrogram representation of hierarchical links between experiments (Fig. 4). Component analysis allowed us to easily visualize the fact that expression of some genes significantly increased (*Masp1*, *Chgn*, *Ust*) or decreased

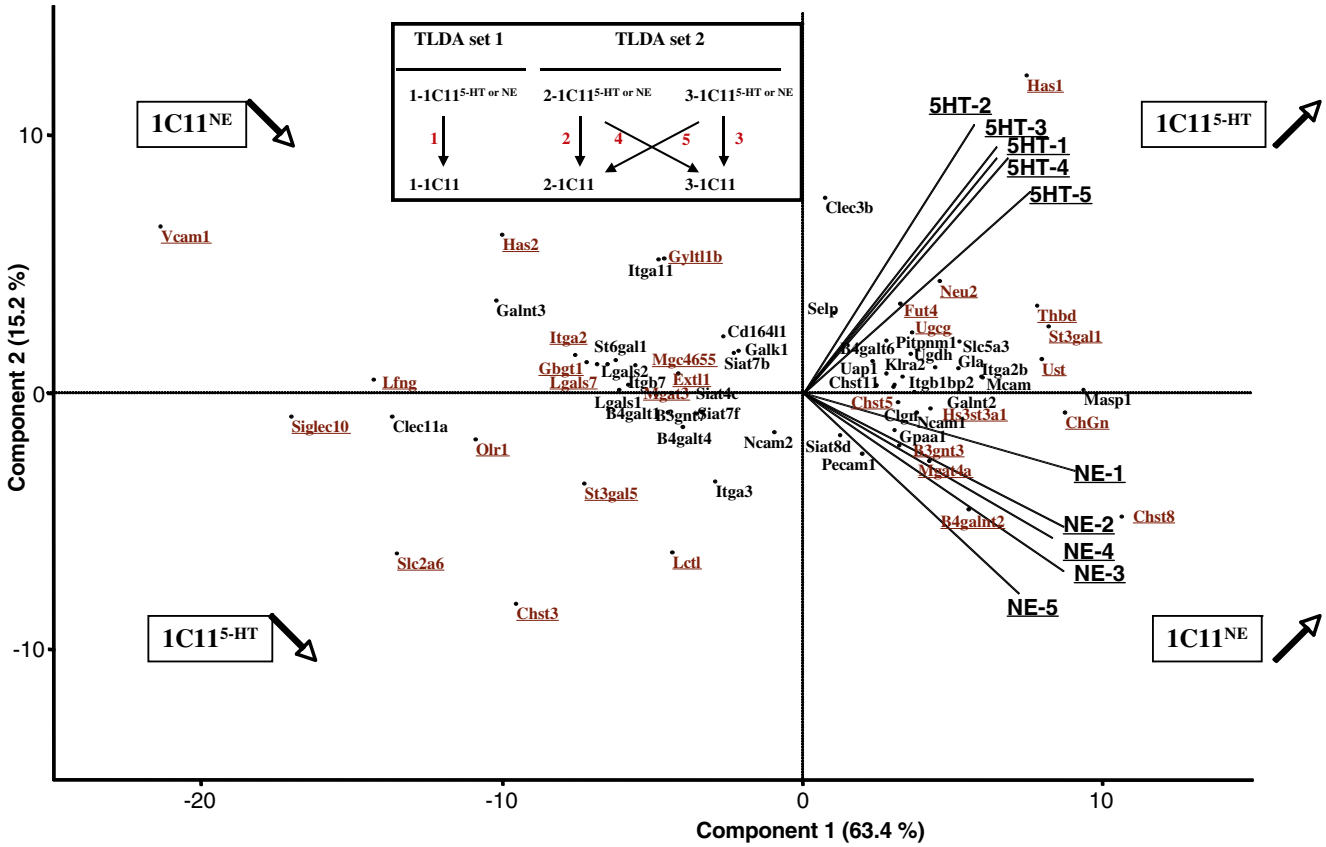

Fig. 3 Glycosylation-related gene expression profile in 1C11$^{5\text{-HT}}$ and 1C11^{NE} differentiated cells relative to undifferentiated 1C11 cells are plotted according to the plan defined by the two first principal components, PC1 and PC2. The PC1 axis corresponds to the gradient of gene expression occurring in both 1C11$^{5\text{-HT}}$ or 1C11^{NE} pathways. Each vector numbered 5HT 1 to 5 and NE 1 to 5, respectively, represents the orientation for genes, which increased along each of the pathways in each experiment. In the opposite direction of these vectors are found genes, whose expression diminished in each pathway. A schematic representation of the experimental conditions is shown in the *inset*. Genes whose expression has been controlled by PCR appear in *red* and are *underlined*

(*Siglec 10*, *Clec11a*, *Lfng*) in both differentiation states, when positioned along the PC1 axis (Fig. 3). Expression of other genes appeared to be specifically regulated in only one of the bioaminergic programs. This is illustrated by the over-expression of *Has1* gene, in 1C11$^{5\text{-HT}}$ cells and *Chst8*, in 1C11^{NE} cells or a decrease of expression of *Chst3*, in 1C11$^{5\text{-HT}}$ cells and *Has2,* in 1C11^{NE} cells.

Values corresponding to fold changes in serotonergic (1C11$^{5\text{-HT}}$/1C11) and noradrenergic (1C11^{NE}/1C11) differentiation states, as well as identity and function of the differentially expressed genes, are listed in Table 2 for the 22 stimulated genes and for the 22 genes with a reduced expression. As already mentioned, we only selected genes with a four-fold variation and a reliable statistical confidence (Student test p value <0.05). In some cases, such as for instance *Mgat4a* expression, the p Student was high due to missing data, but the results were nevertheless given in Table 2 when revealed to be significantly over- or under-expressed by RT-PCR (see below and Fig. 5). The identified genes revealed that variations of expression levels of several glycosyltransferases involved in building up of glycoconjugates occurred during 1C11 neuronal differentiation. This covers *N*-glycan, *O*-glycan and glycosaminoglycan (GAG) synthesis but also sphingolipid and ganglioside pathways among which were found enzymes adding hexosamine (*GlcNAcT*, *GalNAcT*), sialic acid (*SiaT*), or hexose such as fucose (*FucT*) and glucose (*Ugph*). In the case of GAG-metabolism, variations of glycosylation-related gene expression also included specific enzymes involved in formation of hyaluronan (*Has*) or the disaccharides specific of heparan or chondroitin (*Ugdh*, *Ext*). Interestingly, modification of sulfotransferases expression (*Chst, Ust*) known to be important in proteoglycan remodeling [34] appeared to be quite regulated during 1C11 neuronal differentiation. Expression of genes participating in sugar transport (*Slc*) or with carbohydrate specificities such as lectins (*Siglec*, *galectin*) or adhesion molecules (*Mcam*, *Itga*), was also affected.

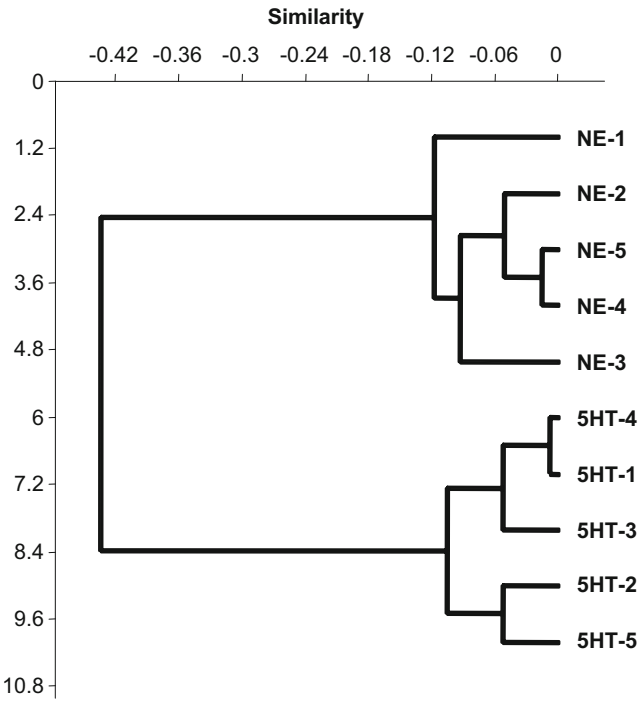

Fig. 4 Dendrogram representation of the hierarchical links between the ten combinations of relative gene expression obtained by TLDA (five experiments in the two differentiation pathways, $1C11^{5\text{-HT}}$ and $1C11^{NE}$)

Confirmation by RT-PCR of differential expression of glycosylation-related genes

Although not used for quantitative expression measurement, the differential expression of genes selected by TLDA was controlled using an RT-PCR method. In addition to visualize the relative expression of genes in each cell state (1C11, $1C11^{5\text{-HT}}$ and $1C11^{NE}$), it was expected to add information about the expression level of glycosylation genes in 1C11 precursor cells serving as reference in microarray analysis. For instance, as shown in Fig. 5, two genes, *St3gal1* and *Chgn*, which were shown in Table 2 to exhibit many fold increases in both serotonergic (x +9.4 and x +8.9 respectively) and noradrenergic (x +5.3 and x +19.3) pathways, were indeed found by RT-PCR to be up-regulated in bioaminergic cells but, their levels of expression in 1C11 precursor cells were quite different. While *St3gal1* was already well detected in 1C11 precursor cells, *Chgn* was undetectable in the undifferentiated state (Fig. 5a). Such variations of the basal level of gene expression in 1C11 had implication for RT-PCR gene expression detection in the differentiated states. For instance, although being up-regulated during bioaminergic differentiation, *Ust* and *Chst5* transcripts, which were not visible in 1C11 samples were hardly detectable in differentiated neuronal cells. The complementarity of the two methods was also evidenced in the case of *Chst8*, whose expression was not significantly altered in serotonergic cells (x +2,5), but highly upregulated in $1C11^{NE}$ cells (x +350). Expression of this gene was detected by RT-PCR in the noradrenergic cells at high amount but was visible neither in 1C11 nor in the serotonergic derived cells.

Among genes exhibiting a clear reduction of expression in both $1C11^{5\text{-HT}}$ and $1C11^{NE}$ neuronal cells, such as *Chst3* (−22 and −250 fold respectively), *Siglec10* (−17 and −25 fold) and *Vcam1* (−7 and −650 fold), *Chst3* and *Siglec10* appeared, by RT-PCR analysis, to be completely switched off in both pathways, while *Vcam1*, which was expressed in high amount in 1C11 cells, was still detectable although clearly diminished in $1C11^{NE}$ differentiated cells (Fig. 5b). While most of the changes seen by TLDA were confirmed by RT-PCR, some differences were observed, but only in a few cases. This could be explained by different sensitivities of the techniques or differences in the design of the sets of primer sequences used for RT-PCR amplification that must differ from the primers of unknown sequences provided for TLDA by the manufacturer.

As a whole, these observations demonstrate that important variations exist in the basal expression levels of different glycosylation-related genes in 1C11 precursor cells. RT-PCR analysis clearly confirmed the specific regulation of glycosylation gene expression during serotonergic and noradrenergic differentiation. Some genes are specifically over (*Chgn*) or under (*Chst3*) expressed in both bioaminergic differentiation pathways, while others have their expression modified in only one of these neuronal pathways. This is the case for *Chst8* which is over-expressed only in $1C11^{NE}$ cells or for *Fut4* in $1C11^{5\text{-HT}}$ cells. Interestingly, some glycosylation-related genes appeared to be induced or shut off during bioaminergic programs.

Impact of variation of glycosylation-related genes during 1C11 neuronal differentiation on PrP^C *N*-glycans and GAG potential partners

Since expression of genes involved in some *N*-glycosylation steps was modified during neuronal differentiation concomitantly with variation of *N*-glycan moieties carried by PrP^C, we then checked by ELISA if some structures specifically recognized by lectins could be detected on PrP^C depending on 1C11 differentiation states. We extrapolated the quantity of PrP^C in cell lysates of each differentiated state (Fig. 6a), from titration curves obtained by PrP^C captured-ELISA. Lectin reactivities were then compared on PrP^C from 1C11 cells and their serotonergic and noradrenergic progenies. While little differences were observed with Mal1 and VV1, we observed a higher

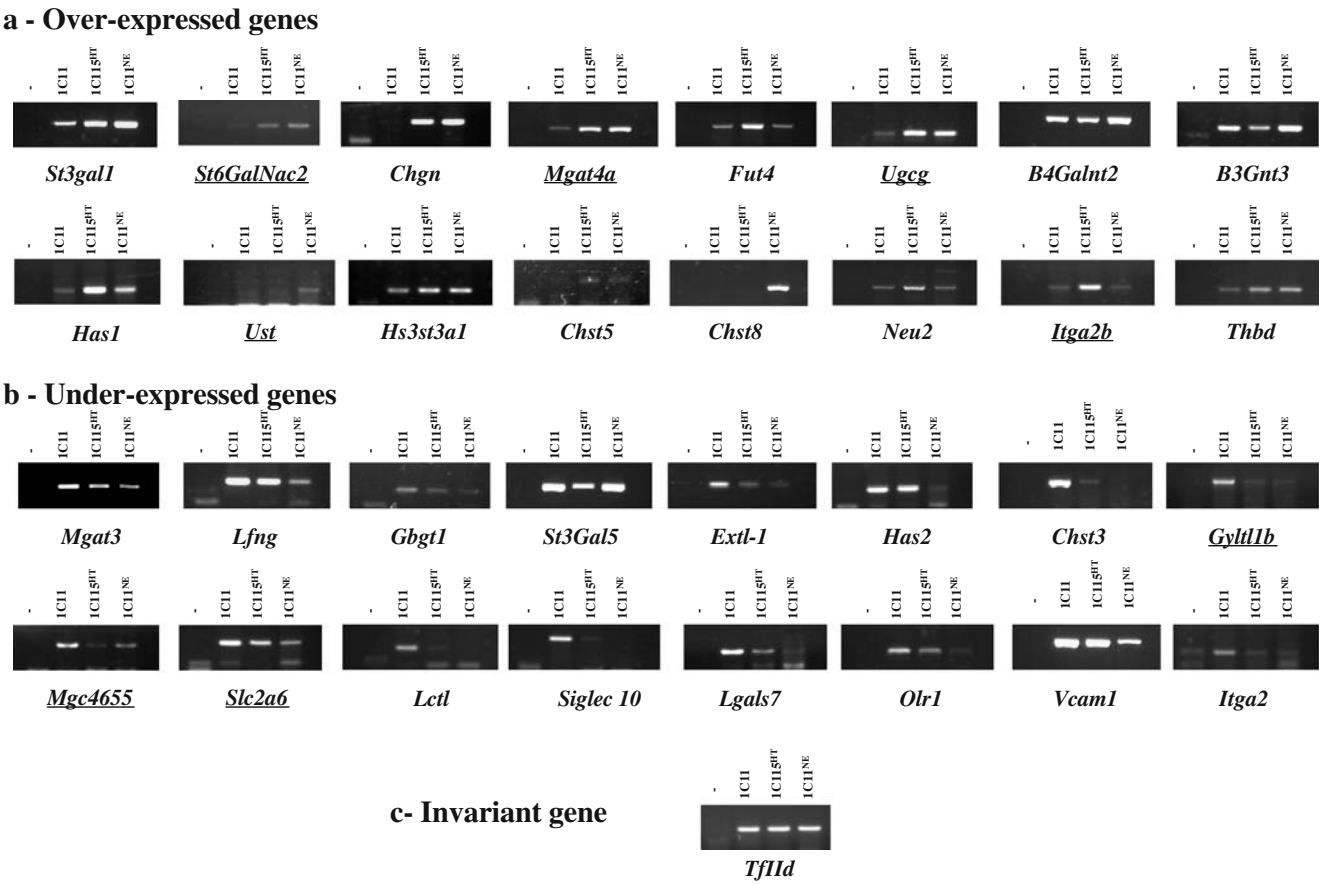

Fig. 5 RT-PCR amplification of different glycosylation-related genes was performed with cDNA of 1C11, $1C11^{5\text{-HT}}$ or $1C11^{NE}$ cells. Negative control (*minus symbol*) is included for each primer set tested. The name of the genes is indicated under each agarose gel panel. Genes are organized according to the table order: in **a**, genes exhibiting enhanced expression and in **b**, genes with decreased expression. As in TLDA the *TfIId* transcription factor was used as an internal control of amplification for invariant gene expression. The genes whose expression differed from the TLDA results are *underlined* (compared with Table 2 and Fig. 4)

reactivity of WGA on PrP^C of $1C11^{5\text{-HT}}$ and $1C11^{NE}$ than on the one of 1C11 lysates (Fig. 6b). Since WGA is reacting with GlcNAc structures, this lectin reactivity may reflect antennation levels. This is in agreement with the shift of PrP^C species towards higher molecular mass corresponding to more complex glycan structures carried by PrP^C in differentiated cells. Although of limited amplitude, another increased reactivity was detected for

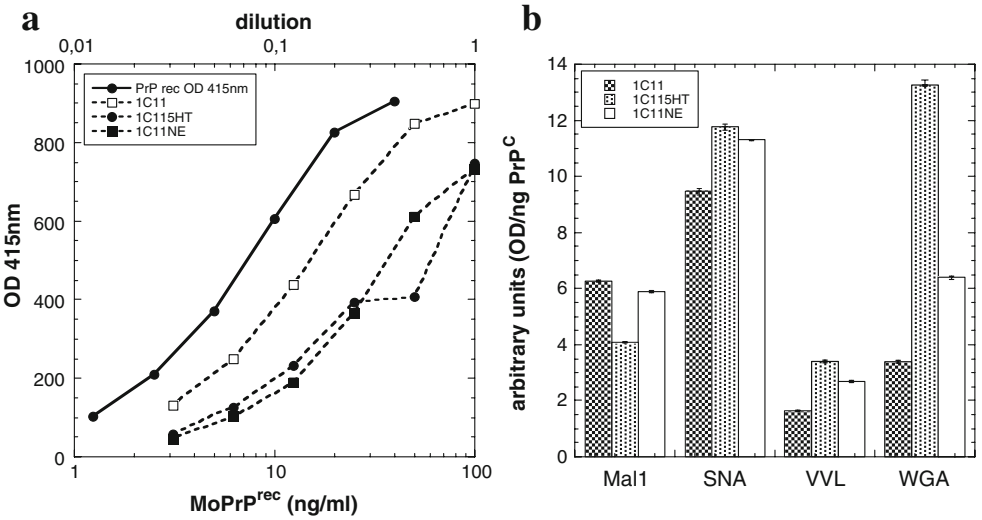

Fig. 6 In **a** are represented the titration curves of PrP^C obtained by ELISA capture. The *bottom X axis* corresponds to dilution of the recombinant mouse PrP (*plain curve*), while *X axis at the top of the curve* corresponds to dilutions (*dotted curves*) of 1C11 (*empty circles*), $1C11^{5\text{-HT}}$ (*black circle*) and $1C11^{NE}$ (*black square*) cell lysate. Lectin reactivities monitored on captured PrP^C from 1C11 (*black bars*), $1C11^{5\text{-HT}}$ (*grey bars*) and $1C11^{NE}$ (*white bars*) lysates are shown in **b**

SNA binding on PrP^C of bioaminergic differentiated cells. This is consistent with an augmentation of the number of sialic acid residues, also supported by the more acidic isoforms of PrP^C observed in 2D-gel (Fig. 2), which could result from an increase in antennation of *N*-glycans in differentiated cells as well as from a higher sialyltransferase activity.

We also tested whether variations relating to GAG synthesis that are summarized in Table 3, could lead to significant variation of the sulfated GAG during 1C11 neuronal differentiation. The methodology we used allowed us to measure, in the first instance, the amount of all sulfated GAGs present in each cell extracts. These sulfated GAGs include chondroitin sulfate (CS), dermatan sulfate (DS, also named chondroitin sulfate B), keratan sulfate (KS), heparan sulfate (HS). Keratan sulfate are mainly present in cornea, cartilage, and bone, and may be considered as insignificant in the 1C11 neuronal model. In a second instance, a deaminative cleavage with nitrous acid was applied to the samples in order to eliminate HS and allowed the measurement of CS only. As shown in Fig. 7a, we detected a higher quantity of total sulfated GAG in $1C11^{NE}$ cells, which was mainly due to an increase in chondroitin sulfate (CS). Of note, *Chst8* transcripts encoding a sulfotransferase adding a sulfate to position 4 of GalNAc, were up-regulated only in these noradrenergic neuronal cells, concomitant to a shut off of *Chst3* involved in sulfatation to position 6 of GalNAc. Whereas no significant variation of total sulfated GAG was measured in $1C11^{5\text{-HT}}$ cells, the proportion of chondroitin sulfate (CS) increased in these cells (Fig. 7b).

Altogether, these results support the idea that, the variation of gene expression occurring during neuronal differentiation may alter both *N*-glycans carried by PrP^C but also PrP^C potential partners such as the GAG associated to membrane of extracellular matrix proteoglycans.

Discussion

Differential PrP^C glycosylation has been documented in cell lines of different origins, but also in different organs, interestingly, depending on brain regions in mouse and human species [18, 19, 35, 36]. Here we showed that an heterogeneity of PrP^C glycopatterns was associated to bioaminergic differentiation programs. This was illustrated by the differences of the 1D- and 2D electrophoretic profiles of PrP^C in $1C11^{5\text{-HT}}$ serotonergic and $1C11^{NE}$ noradrenergic cells both derived from the same 1C11 neuroepithelial precursor line [21]. Improved knowledge on the diversity of glycosylation pathways recently led to development of glycomic approaches [24]. Using such a transcriptomic analysis allowed us to make a link between differential heterogeneity of PrP^C glycoforms and variation of glycosylation-related gene expression during bioaminergic neuronal differentiation.

Out of the 375 tested genes, 44 different transcripts encoding proteins were found to be differentially expressed in bioaminergic neuronal cells using 1C11 precursor cells as reference. Some of the variations affected genes involved in *N*-glycan synthesis that could contribute to the higher molecular weights and more acidic forms associated to the electrophoretic profiles of glycosyated PrP^C in bioaminergic neuronal cells. Indeed an upregulation of *Mgat4a*, a GlcNAc-transferase involved in formation of triantenary *N*-glycan structures occurred in $1C11^{5\text{-HT}}$ and $1C11^{NE}$ cells. Concomitantly, a down regulation of *Mgat3* which elongates the central mannose of the tri-mannosyl core of the *N*-

Table 3 Variations of expression of genes involved in GAG synthesis

Gene name	Function	Level of expression in		
		1C11	$1C11^{5\text{-HT}}$	$1C11^{NE}$
Chgn	GalNAc-transferase synthesis of the linker of chondroitin	−	++ (x 9)	++ (x 19)
Extl1	GalNAc-transferase synthesis of disaccharide unit of GAG	++	+/− (x −2)	− (x −3)
Has1	Hyaluronan synthase 1 synthesis of HA GAG substrate	+	+++ (x 96)	++ (p NS)
Has2	Hyaluronan synthase 2 synthesis of HA GAG substrate	++	++ (p NS)	− (x −30)
Hs3st3a1	GlcN-Sulfotransferase sulfatation of HSPG	+	++ (x 5)	++ (x 5)
Ust	Uronyl-Sulfotransferase sulfatation of CSPG	−	++ (x 10)	++ (x 10)
Chst3	Chondroitin-6-Sulfotransferase sulfatation of CSPG	+++	+/− (x −22)	− (x −200)
Chst5	GlcNAc-Sulfotransferase sulfatation of diverse glycans	−	+ (x 4)	+ (x 4)
Chst8	GalNAc-Sulfotransferase sulfatation of diverse glycans	−	− (p NS)	+++ (x 300)

− (not visible) and +/− to +++ (low to high detection) as extrapolated from Fig. 6. The fold change (mean RQ values from TLDA) are into brackets and are not given (*p* NS) when the *p* student was no significant

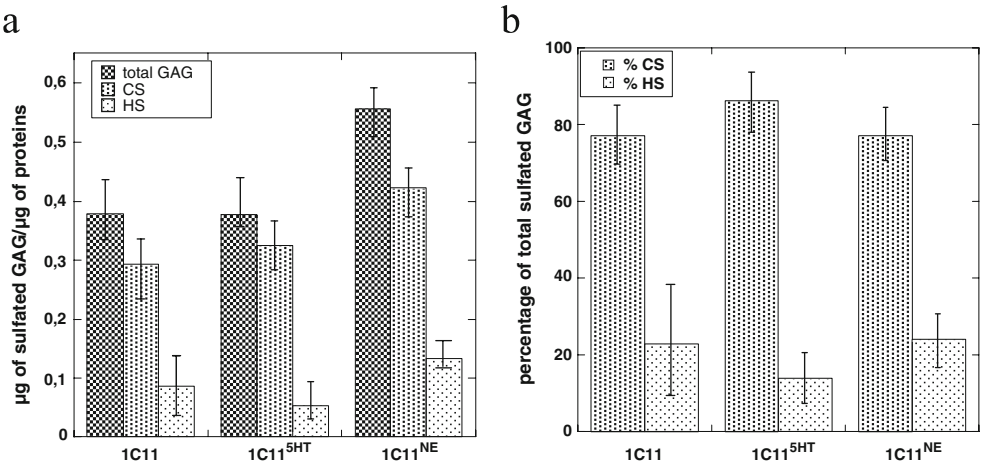

Fig. 7 Panel **a** shows the relative quantity of sulfated GAG either total (*black bar*) chondroitin (*grey bar*) or heparan (*white bar*) in the different 1C11 neuronal pathways. The percentage of CS and HS is shown in **b**

glycan was observed. Since a central GlcNAc addition blocks further antennation of the two lateral residues of the tri-mannosylated core, a decreased expression of *Mgat3* should favor *N*-glycan branching [3]. In such a scenario no higher sialyltransferase activities are required to enhance the sialylation levels of *N*-glycans. However, the *St3gal1* gene belonging to this transferase family [37], was upregulated in 1C11 bioaminergic cells and could enhance *N*-glycan sialylation. A modulation of glycosyltransferase activities affecting PrP^C glycosylation was also documented by changes in lectin reactivities to GlcNAc and to sialic acid on PrP^C, according to 1C11 neuronal differentiation state.

Our observation of PrP^C glycopatterns varying with bioaminergic programs, points to a regulation of glycosylation-related gene expression during neuronal differentiation. This is of interest in view of accumulating evidences for an essential role of various glycoconjugates in the development of the central nervous system [25]. Here, the 44 genes exhibiting a significant expression fold change in bioaminergic neuronal cells were involved in *N*-glycosylation, *O*-glycosylation, glycosaminoglycan, and glycosphingolipid metabolism, or in the synthesis of glycoproteins interacting with carbohydrate moieties (lectins, adhesion molecules). Some of the genes exhibited higher or lower transcription levels in either the serotonergic or noradrenergic pathway, while others were altered in both of these bioaminergic pathways. For instance, the expression level of the fucosyltransferase *Fut4* only increased in the $1C11^{5\text{-HT}}$ serotonergic progenies and a strong upregulation of the sialidase *Neu2* was also observed in these cells while a GalNAc (*B4galnt2*) and a GlcNAc (*B3gnt3*) transferase increased in $1C11^{NE}$ cells. For the sialyltransferase, *St3gal1*, the C-lectin, *Masp1* and the receptor, *Thbd*, they were upregulated in both $1C11^{5\text{-HT}}$ and $1C11^{NE}$ bioaminergic pathways. A similar observation apply to downregulated genes. For instance, expression of the sialyltransferase *St3gal5* was diminished in serotonergic cells, the hyaluronidase *Has2* in noradrenergic ones and the glycosyltransferase *Lfng* or the chondroitin sulfate *Chst3* in both bioaminergic pathways. Most of these tightly regulated variations were confirmed by RT-PCR, which also allowed to determine the basal level of gene expression in 1C11 precursor cells. It revealed that some RNA transcripts, not detectable in 1C11, were induced during bioaminergic differentiation, such as *Chst8* in $1C11^{NE}$ cells or *Chgn,* in both programs. It also revealed a nearly switching off of some genes, as is the case for the *Siglec 10* lectin or *Chst3*, undetectable in both pathways. Of note, fold changes in gene expression appeared surprisingly high, probably due to the homogeneity of the 1C11 derived neuronal cell populations.

Our data, together with the diversity of glycoconjugates, highlight the degree of complexity of carbohydrate regulation during neuronal differentiation. In this respect, the CNS stand for a good model of investigation of carbohydrate implications in neuronal development and plasticity. For instance, sialylation, in particular the polysialic acid modifying the neural cell adhesion molecule, NCAM, have been proposed to play a major role in brain development [38]. While α2–8 NeuA linkages are involved in polySia formation, other sialyltransferase activities are also regulated in neuronal cells, favoring α2–3 linkages at the expense of α2–6 linkages on glycoprotein-associated carbohydrates [25]. Our findings of an increased expression of *St3gal1* (responsible for α2–3 NeuA linkage), in both $1C11^{5\text{-HT}}$ and $1C11^{NE}$ cells, or a decrease of *St6gal1* (responsible for sialylation in α2–6), in noradrenergic cells, is consistent with a tight regulation of sialyltransferase activities during neuronal differentiation. Interestingly, some glycosyltransferases may be involved in several glycosylation metabolic pathways also involving glycolipids. This is the case for transferases orchestrating sialic acid, GlcNAc and Gal additions on N-glycans, which also contribute to regulation of ganglioside structures in the nervous system [39, 40]. Glycosphingolipids and in particular gangliosides are also important players for cell signaling in neuronal cells [23].

In this context *St3gal1*, which was up regulated in both bioaminergic pathways not only modifies *N*-glycans, but also gangliosides. Another sialyltransferase, *St3gal5*, specific of GM3 synthesis and highly expressed in 1C11 and $1C11^{NE}$ noradrenergic cells, was downregulated only in $1C11^{5\text{-}HT}$ serotonergic cells.

Carbohydrates are hydrophilic structures exposed to the surface of the molecules to which they are attached, creating epitopes serving as modulators through interaction with lectins or specific receptors. It has recently been demonstrated that increasing *N*-glycan branching, increased cell surface association of growth promoting receptors with the galectin 3 lectin and that branching level could regulate transition from growth to arrest [41]. It is noticeable that expression of enzymes involved in N-glycan antennation were modulated in the 1C11 neuronal model. Interestingly, some sugar epitopes (Le^X, HNK1) are shared by different types of glycoconjugates and some neural proteins like NCAM and L1 have dual characteristics by both being highly glycosylated, and having lectin-like specificities [25]. In the 1C11 bioaminergic cells some enzymes generating Le^X epitopes or receptors involved in carbohydrate interactions are highly upregulated (*Fut4*, *Masp1*, *Clec3b*, *Itga2b*, *Thbd*), while some others are downregulated (*Lgals7*, *Olr1*, *Vcam1*, *Itga2*) with a near complete switch off of the *Siglec10* lectin. Glycoconjugates are thought to be involved in the regulation of many functions through networks of interactions. In neuronal cells, such a regulation will recruit carbohydrate structures on plasma membrane and in the extracellular matrix (ECM). Considering their large distribution at the cell-ECM interface, GAG may interact with many proteins and modulate their activities [42]. Proteoglycans are now well recognized as regulators of neuronal functions [26]. Interestingly, an additional level of GAG diversity relates to the type of sulfate linkages. It has been proposed that chondroitin sulfate proteoglycans (CSPG) could have a role in neuronal plasticity and in regeneration of injured or diseased neurons [34], and heparan sulfate proteoglycans (HSPG) in axon guidance [43]. In the 1C11 bioaminergic differentiation model, important variations of gene expression affect enzymes involved in GAG synthesis and sulfation as exemplified in Table 3. Although the amount of sulfated GAGs was increased in noradrenergic cells, it is difficult to correlate all these data. Indeed we have analyzed the expression level of only part of the genes involved in GAGs metabolism (synthesis and sulfation), and sulfated GAGs quantification does not discriminate between a change in the amount of equally sulfated GAGs or a change in sulfation of an equal amount of GAGs. However, it's clear that the ECM compositions of the two bioaminergic differentiated progenies will be different: $1C11^{NE}$ noradrenergic cells presenting a higher amount of sulfated GAGs or an equal amount of highly sulfated GAGs. Much is still to be learned about glycosylations, and glycomics approach represents a new efficient tool to study the role and regulation of glycoconjugates. While this work was in progress, a microarray analysis was conducted by Smith *et al.* [44] to compare the glycogenome of cerebellar neurons at two different stages of post-natal development. Corroborating our data, the authors of the study described regulated expression of sialyltransferases, GalNAc-transferases, and sulfotransferases in their neuronal model.

The observed variations of glycosylation-related gene expression by affecting many pathways may have an impact on neuronal functions. In the case of PrP^C, modulation of carbohydrate structures could directly participate in its neurospecificity, but could also affect its interacting partners, thereby modulating the composition of membrane protein complexes. In the context of previously described interaction of PrP^C with laminin through heparan sulfate molecules [8, 11], it is of interest that gene expression related to GAG synthesis appeared to be regulated during 1C11 neuronal differentiation. Direct interactions of PrP^C with GAG [45], but also with different lectins [46], have also been inferred from *in vitro* studies. Recent studies suggest that expression of Le^X and sLe^X epitopes by PrP^C *N*-glycans could be ligands of selectins [47]. Furthermore, intriguing aspects of prion diseases relate to the multiplicity of strains harboring their own specific properties and also, to the stability of strain characteristics maintained upon transmission. This suggests that a unique protein may exist under different conformations responsible for variable pathologies [48]. Recent data support the hypothesis of an involvement of prion glycosylation in strain diversity [19, 49, 50]. Specifc brain targeting of prion strains relating to the various lesion profiles associated to different prion disorders, could depend on glycosylation of both, the infecting scrapie strain and the host PrP^C [50–55]. Alternatively prion diseases could affect host glycosylation [56]. Transcriptomic analyses have been performed to investigate the effect of prion infection on cell metabolism [57–60] and we previously reported that regulation of enzymes involved in CSPG metabolism was affected in scrapie infected neuroblastoma cells [61].

In conclusion, our data highlight a clear change during bioaminergic differentiation in the expression of genes involved in many different aspects of glycoconjugate metabolism which may account for PrP^C glycosylation differences. Further investigations should allow to gain insight into changes in PrP^C *N*-glycans in this neuronal model and their implications in PrP^C neuronal function. Moreover, the 1C11 cell line, which was recently shown to have the capacity to replicate prion strains [62], could help understand some aspects of glycosylation in relation to prion infection.

Acknowledgements The authors wish to thank Wendy Houssin for careful reading of the manuscript. We are grateful to Fabrice Dupuy, Lionel Forestier and Raymond Julien for the implementation and support of the TLDA technology. This work was supported by the "Conseil Régional du Limousin" and by "INRA" (Institut National de la Recherche Agronomique), "CNRS" and "Institut Pasteur" and by grants from "GIS Infection à Prion".

References

1. Prusiner, S.B.: Prions. Proc. Natl. Acad. Sci. U.S.A **95**, 13363–13383 (1998). doi:10.1073/pnas.95.23.13363
2. Haraguchi, T., Fisher, S., Olofsson, S., Endo, T., Groth, D., Tarentino, A., Borchelt, D.R., Teplow, D., Hood, L., Burlingame, A., et al.: Asparagine-linked glycosylation of the scrapie and cellular prion proteins. Arch. Biochem. Biophys **274**, 1–13 (1989). doi:10.1016/0003-9861(89)90409-8
3. Rudd, P.M., Endo, T., Colominas, C., Groth, D., Wheeler, S.F., Harvey, D.J., Wormald, M.R., Serban, H., Prusiner, S.B., Kobata, A., Dwek, R.A.: Glycosylation differences between the normal and pathogenic prion protein isoforms. Proc. Natl. Acad. Sci. U.S.A **96**, 13044–13049 (1999). doi:10.1073/pnas.96.23.13044
4. Stimson, E., Hope, J., Chong, A., Burlingame, A.L.: Site-specific characterization of the N-linked glycans of murine prion protein by high-performance liquid chromatography/electrospray mass spectrometry and exoglycosidase digestions. Biochemistry **38**, 4885–4895 (1999). doi:10.1021/bi982330q
5. Rudd, P.M., Wormald, M.R., Wing, D.R., Prusiner, S.B., Dwek, R.A.: Prion glycoprotein: structure, dynamics, and roles for the sugars. Biochemistry **40**, 3759–3766 (2001). doi:10.1021/bi002625f
6. Pan, T., Li, R., Wong, B.S., Liu, T., Gambetti, P., Sy, M.S.: Heterogeneity of normal prion protein in two-dimensional immunoblot: presence of various glycosylated and truncated forms. J. Neurochem **81**, 1092–1101 (2002). doi:10.1046/j.1471-4159.2002.00909.x
7. Jackson, G.S., Murray, I., Hosszu, L.L., Gibbs, N., Waltho, J.P., Clarke, A.R., Collinge, J.: Location and properties of metal-binding sites on the human prion protein. Proc. Natl. Acad. Sci. U.S.A **98**, 8531–8535 (2001). doi:10.1073/pnas.151038498
8. Hundt, C., Peyrin, J.M., Haik, S., Gauczynski, S., Leucht, C., Rieger, R., Riley, M.L., Deslys, J.P., Dormont, D., Lasmezas, C.I., Weiss, S.: Identification of interaction domains of the prion protein with its 37-kDa/67-kDa laminin receptor. EMBO J **20**, 5876–5886 (2001). doi:10.1093/emboj/20.21.5876
9. Schmitt-Ulms, G., Legname, G., Baldwin, M.A., Ball, H.L., Bradon, N., Bosque, P.J., Crossin, K.L., Edelman, G.M., DeArmond, S.J., Cohen, F.E., Prusiner, S.B.: Binding of neural cell adhesion molecules (N-CAMs) to the cellular prion protein. J. Mol. Biol **314**, 1209–1225 (2001). doi:10.1006/jmbi.2000.5183
10. Graner, E., Mercadante, A.F., Zanata, S.M., Forlenza, O.V., Cabral, A.L., Veiga, S.S., Juliano, M.A., Roesler, R., Walz, R., Minetti, A., Izquierdo, I., Martins, V.R., Brentani, R.R.: Cellular prion protein binds laminin and mediates neuritogenesis. Brain Res. Mol. Brain Res **76**, 85–92 (2000). doi:10.1016/S0169-328X(99)00334-4
11. Warner, R.G., Hundt, C., Weiss, S., Turnbull, J.E.: Identification of the heparan sulfate binding sites in the cellular prion protein. J. Biol. Chem **277**, 18421–18430 (2002). doi:10.1074/jbc.M110406200
12. Kanaani, J., Prusiner, S.B., Diacovo, J., Baekkeskov, S., Legname, G.: Recombinant prion protein induces rapid polarization and development of synapses in embryonic rat hippocampal neurons in vitro. J. Neurochem **95**, 1373–1386 (2005). doi:10.1111/j.1471-4159.2005.03469.x
13. Krebs, B., Dorner-Ciossek, C., Schmalzbauer, R., Vassallo, N., Herms, J., Kretzschmar, H.A.: Prion protein induced signaling cascades in monocytes. Biochem. Biophys. Res. Commun **340**, 13–22 (2006)
14. Mouillet-Richard, S., Ermonval, M., Chebassier, C., Laplanche, J.L., Lehmann, S., Launay, J.M., Kellermann, O.: Signal transduction through prion protein. Science **289**, 1925–1928 (2000). doi:10.1126/science.289.5486.1925
15. Mouillet-Richard, S., Schneider, B., Pradines, E., Pietri, M., Ermonval, M., Grassi, J., Richards, J.G., Mutel, V., Launay, J.M., Kellermann, O.: Cellular prion protein signaling in serotonergic neuronal cells. Ann. N. Y. Acad. Sci **1096**, 106–119 (2007). doi:10.1196/annals.1397.076
16. Schneider, B., Mutel, V., Pietri, M., Ermonval, M., Mouillet-Richard, S., Kellermann, O.: NADPH oxidase and extracellular regulated kinases 1/2 are targets of prion protein signaling in neuronal and nonneuronal cells. Proc. Natl. Acad. Sci. U.S.A **100**, 13326–13331 (2003). doi:10.1073/pnas.2235648100
17. Linden, R., Martins, V.R., Prado, M.A., Cammarota, M., Izquierdo, I., Brentani, R.R.: Physiology of the prion protein. Physiol. Rev **88**, 673–728 (2008). doi:10.1152/physrev.00007.2007
18. Beringue, V., Mallinson, G., Kaisar, M., Tayebi, M., Sattar, Z., Jackson, G., Anstee, D., Collinge, J., Hawke, S.: Regional heterogeneity of cellular prion protein isoforms in the mouse brain. Brain **126**, 2065–2073 (2003). doi:10.1093/brain/awg205
19. DeArmond, S.J., Qiu, Y., Sanchez, H., Spilman, P.R., Ninchak-Casey, A., Alonso, D., Daggett, V.: PrPc glycoform heterogeneity as a function of brain region: implications for selective targeting of neurons by prion strains. J. Neuropathol. Exp. Neurol **58**, 1000–1009 (1999). doi:10.1097/00005072-199909000-00010
20. Ermonval, M., Mouillet-Richard, S., Codogno, P., Kellermann, O., Botti, J.: Evolving views in prion glycosylation: functional and pathological implications. Biochimie **85**, 33–45 (2003). doi:10.1016/S0300-9084(03)00040-3
21. Mouillet-Richard, S., Mutel, V., Loric, S., Tournois, C., Launay, J.M., Kellermann, O.: Regulation by neurotransmitter receptors of serotonergic or catecholaminergic neuronal cell differentiation. J. Biol. Chem **275**, 9186–9192 (2000b). doi:10.1074/jbc.275.13.9186
22. Mouillet-Richard, S., Pietri, M., Schneider, B., Vidal, C., Mutel, V., Launay, J.M., Kellermann, O.: Modulation of serotonergic receptor signaling and cross-talk by prion protein. J. Biol. Chem **280**, 4592–4601 (2004). doi:10.1074/jbc.M406199200
23. Allen, J.A., Halverson-Tamboli, R.A., Rasenick, M.M.: Lipid raft microdomains and neurotransmitter signalling. Nat. Rev. Neurosci **8**, 128–140 (2007). doi:10.1038/nrn2059
24. Comelli, E.M., Head, S.R., Gilmartin, T., Whisenant, T., Haslam, S.M., North, S.J., Wong, N.K., Kudo, T., Narimatsu, H., Esko, J.D., Drickamer, K., Dell, A., Paulson, J.C.: A focused microarray approach to functional glycomics: transcriptional regulation of the glycome. Glycobiology **16**, 117–131 (2005). doi:10.1093/glycob/cwj048
25. Kleene, R., Schachner, M.: Glycans and neural cell interactions. Nat. Rev. Neurosci **5**, 195–208 (2004). doi:10.1038/nrn1349
26. Schwartz, N.B., Domowicz, M.: Proteoglycans in brain development. Glycoconj. J **21**, 329–341 (2004). doi:10.1023/B:GLYC.0000046278.34016.36
27. Clausse, B., Fizazi, K., Walczak, V., Tetaud, C., Wiels, J., Tursz, T., Busson, P.: High concentration of the EBV latent membrane protein 1 in glycosphingolipid-rich complexes from both epithelial and lymphoid cells. Virology **228**, 285–293 (1997). doi:10.1006/viro.1996.8380
28. Sobue, K., Kanda, K.: Alpha-actinins, calspectin (brain spectrin or fodrin), and actin participate in adhesion and movement of growth cones. Neuron **3**, 311–319 (1989). doi:10.1016/0896-6273(89)90255-9

29. Milhiet, P.E., Vacherot, F., Caruelle, J.P., Barritault, D., Caruelle, D., Courty, J.: Upregulation of the angiogenic factor heparin affin regulatory peptide by progesterone in rat uterus. J. Endocrinol **158**, 389–399 (1998). doi:10.1677/joe.0.1580389
30. Tusher, V.G., Tibshirani, R., Chu, G.: Significance analysis of microarrays applied to the ionizing radiation response. Proc. Natl. Acad. Sci. U.S.A **98**, 5116–5121 (2001). doi:10.1073/pnas.091062498
31. Hammer, O., Harper, D.A.T., Ryan, P.D.: PAST: Paleontological Statistics Software Package for Education and Data Analysis. Palaeontologia Electronica. http://palaeo-electronica.org/2001_1/past/issue1_01.htm, **4**(1), 9pp. (2001)
32. Sokal, R.R., Rohlf, F.J.: Biometry: the principles and practice of statistics in biological research. Freeman, New York (1995), 887 p
33. Barbosa, I., Garcia, S., Barbier-Chassefiere, V., Caruelle, J.P., Martelly, I., Papy-Garcia, D.: Improved and simple micro assay for sulfated glycosaminoglycans quantification in biological extracts and its use in skin and muscle tissue studies. Glycobiology **13**, 647–653 (2003). doi:10.1093/glycob/cwg082
34. Galtrey, C.M., Fawcett, J.W.: The role of chondroitin sulfate proteoglycans in regeneration and plasticity in the central nervous system. Brain Res. Brain Res. Rev **54**, 1–18 (2007). doi:10.1016/j.brainresrev.2006.09.006
35. Kuczius, T., Koch, R., Keyvani, K., Karch, H., Grassi, J., Groschup, M.H.: Regional and phenotype heterogeneity of cellular prion proteins in the human brain. Eur. J. Neurosci **25**, 2649–2655 (2007). doi:10.1111/j.1460-9568.2007.05518.x
36. Monnet, C., Marthiens, V., Enslen, H., Frobert, Y., Sobel, A., Mege, R.M.: Heterogeneity and regulation of cellular prion protein glycoforms in neuronal cell lines. Eur. J. Neurosci **18**, 542–548 (2003). doi:10.1046/j.1460-9568.2003.02777.x
37. Harduin-Lepers, A., Vallejo-Ruiz, V., Krzewinski-Recchi, M.A., Samyn-Petit, B., Julien, S., Delannoy, P.: The human sialyltransferase family. Biochimie **83**, 727–737 (2001). doi:10.1016/S0300-9084(01)01301-3
38. Hildebrandt, H., Muhlenhoff, M., Weinhold, B., Gerardy-Schahn, R.: Dissecting polysialic acid and NCAM functions in brain development. J. Neurochem **103**, 56–64 (2007). doi:10.1111/j.1471-4159.2007.04716.x
39. Wu, A.M.: Carbohydrate structural units in glycosphingolipids as receptors for Gal and GalNAc reactive lectins. Neurochem. Res **27**, 593–600 (2002). doi:10.1023/A:1020263730943
40. Yu, R.K., Bieberich, E., Xia, T., Zeng, G.: Regulation of ganglioside biosynthesis in the nervous system. J. Lipid Res **45**, 783–793 (2004). doi:10.1194/jlr.R300020-JLR200
41. Lau, K.S., Partridge, E.A., Grigorian, A., Silvescu, C.I., Reinhold, V.N., Demetriou, M., Dennis, J.W.: Complex N-glycan number and degree of branching cooperate to regulate cell proliferation and differentiation. Cell **129**, 123–134 (2007). doi:10.1016/j.cell.2007.01.049
42. Sasisekharan, R., Raman, R., Prabhakar, V.: Glycomics approach to structure-function relationships of glycosaminoglycans. Annu. Rev. Biomed. Eng **8**, 181–231 (2006). doi:10.1146/annurev.bioeng.8.061505.095745
43. Lee, J.S., Chien, C.B.: When sugars guide axons: insights from heparan sulphate proteoglycan mutants. Nat. Rev. Genet **5**, 923–935 (2004). doi:10.1038/nrg1490
44. Smith, F.I., Qu, Q., Hong, S.J., Kim, K.S., Gilmartin, T.J., Head, S.R.: Gene expression profiling of mouse postnatal cerebellar development using oligonucleotide microarrays designed to detect differences in glycoconjugate expression. Gene Expr. Patterns **5**, 740–749 (2005). doi:10.1016/j.modgep.2005.04.006
45. Pan, T., Wong, B.S., Liu, T., Li, R., Petersen, R.B., Sy, M.S.: Cell-surface prion protein interacts with glycosaminoglycans. Biochem. J **368**, 81–90 (2002). doi:10.1042/BJ20020773
46. Triantaphyllidou, I.E., Sklaviadis, T., Vynios, D.H.: Detection, quantification, and glycotyping of prion protein in specifically activated enzyme-linked immunosorbent assay plates. Anal. Biochem **359**, 176–182 (2006). doi:10.1016/j.ab.2006.10.002
47. Li, C., Wong, P., Pan, T., Xiao, F., Yin, S., Chang, B., Kang, S.C., Ironside, J., Sy, M.S.: Normal cellular prion protein is a ligand of selectins: binding requires Le(X) but is inhibited by sLe(X). Biochem. J **406**, 333–341 (2007). doi:10.1042/BJ20070186
48. Aguzzi, A., Heikenwalder, M., Polymenidou, M.: Insights into prion strains and neurotoxicity. Nat. Rev. Mol. Cell Biol **8**, 552–561 (2007). doi:10.1038/nrm2204
49. Atkinson, P.H.: Glycosylation of prion strains in transmissible spongiform encephalopathies. Aust. Vet. J **82**, 292–299 (2004). doi:10.1111/j.1751-0813.2004.tb12709.x
50. Khalili-Shirazi, A., Summers, L., Linehan, J., Mallinson, G., Anstee, D., Hawke, S., Jackson, G.S., Collinge, J.: PrP glycoforms are associated in a strain-specific ratio in native PrPSc. J. Gen. Virol **86**, 2635–2644 (2005). doi:10.1099/vir.0.80375-0
51. Moudjou, M., Treguer, E., Rezaei, H., Sabuncu, E., Neuendorf, E., Groschup, M.H., Grosclaude, J., Laude, H.: Glycan-controlled epitopes of prion protein include a major determinant of susceptibility to sheep scrapie. J. Virol **78**, 9270–9276 (2004). doi:10.1128/JVI.78.17.9270-9276.2004
52. Nishina, K.A., Deleault, N.R., Mahal, S.P., Baskakov, I., Luhrs, T., Riek, R., Supattapone, S.: The stoichiometry of host PrPC glycoforms modulates the efficiency of PrPSc formation in vitro. Biochemistry **45**, 14129–14139 (2006). doi:10.1021/bi061526k
53. Priola, S.A., Lawson, V.A.: Glycosylation influences cross-species formation of protease-resistant prion protein. EMBO J **20**, 6692–6699 (2001). doi:10.1093/emboj/20.23.6692
54. Tuzi, N.L., Cancellotti, E., Baybutt, H., Blackford, L., Bradford, B., Plinston, C., Coghill, A., Hart, P., Piccardo, P., Barron, R.M., Manson, J.C.: Host PrP Glycosylation: a major factor determining the outcome of prion infection. PLoS Biol **6**, e100 (2008). doi:10.1371/journal.pbio.0060100
55. Vorberg, I., Priola, S.A.: Molecular basis of scrapie strain glycoform variation. J. Biol. Chem **277**, 36775–36781 (2002). doi:10.1074/jbc.M206865200
56. Hounsell, E.F.: Prions in control of cell glycosylation. Biochem. J **380**, e5–e6 (2004). doi:10.1042/BJ20040657
57. Jin, J.K., Na, Y.J., Song, J.H., Joo, H.G., Kim, S., Kim, J.I., Choi, E.K., Carp, R.I., Kim, Y.S., Shin, T.: Galectin-3 expression is correlated with abnormal prion protein accumulation in murine scrapie. Neurosci. Lett **420**, 138–143 (2007). doi:10.1016/j.neulet.2007.04.069
58. Silveyra, M.X., Cuadrado-Corrales, N., Marcos, A., Barquero, M.S., Rabano, A., Calero, M., Saez-Valero, J.: Altered glycosylation of acetylcholinesterase in Creutzfeldt–Jakob disease. J. Neurochem **96**, 97–104 (2006). doi:10.1111/j.1471-4159.2005.03514.x
59. Sorensen, G., Medina, S., Parchaliuk, D., Phillipson, C., Robertson, C., Booth, S.A.: Comprehensive transcriptional profiling of prion infection in mouse models reveals networks of responsive genes. BMC Genomics **9**, 114 (2008). doi:10.1186/1471-2164-9-114
60. Xiang, W., Hummel, M., Mitteregger, G., Pace, C., Windl, O., Mansmann, U., Kretzschmar, H.A.: Transcriptome analysis reveals altered cholesterol metabolism during the neurodegeneration in mouse scrapie model. J. Neurochem **102**, 834–847 (2007). doi:10.1111/j.1471-4159.2007.04566.x
61. Barret, A., Forestier, L., Deslys, J.P., Julien, R., Gallet, P.F.: Glycosylation-related gene expression in prion diseases: PrPSc accumulation in scrapie infected GT1 cells depends on beta-1,4-linked GalNAc-4-SO4 hyposulfation. J. Biol. Chem **280**, 10516–10523 (2005). doi:10.1074/jbc.M412635200
62. Mouillet-Richard, S., Nishida, N., Pradines, E., Laude, H., Schneider, B., Feraudet, C., Grassi, J., Launay, J.M., Lehmann, S., Kellermann, O.: Prions impair bioaminergic functions through serotonin- or catecholamine-derived neurotoxins in neuronal cells. J. Biol. Chem **283**, 23782–23790 (2008). doi:10.1074/jbc.M802433200